EUROPEAN FUSION DEVELOPMENT AGREEMENT

EFDA–JET–PR(01)114

V.V. Parail

Energy and Particle Transport in Plasmas with Transport Barriers

Energy and Particle Transport in Plasmas with Transport Barriers

V.V. Parail

EURATOM-UKAEA Fusion Association, Culham Science Centre, Abingdon, OX14 3DB, UK

Paper to be submitted for publication in PPCF

ABSTRACT

Up to five regions with different transport properties can be identified in tokamak plasma with edge and internal transport barriers. This includes edge and core barriers, the region near the separatrix, which is dominated by atomic physics, the core plasma (within $0.4 \leq \rho \leq 0.8$, where ¡ is a normalised minor radius) and central part of plasma volume, which is often, dominated by large scale MHD phenomena. An overview of present understanding of the heat and particle transport in these five regions will be given, which includes progress in experimental observations, theory of plasma micro-turbulence and predictive modelling.

1. INTRODUCTION

Understanding of plasma transport is an issue of a paramount importance for the design of a future tokamak power plant. Together with some major MHD instabilities, anomalous transport controls plasma confinement and overall fusion performance. As a result heat, particle and momentum transport of electrons, ions and impurities in tokamaks has been studied both experimentally and theoretically for more than two decades. It has been universally recognised that transport properties vary a lot across the plasma so that it is constructive to subdivide the plasma volume into up to five regions with different transport characteristics. The schematic view of such a division is shown in Figure 1. Starting from the edge, first is the scrape-off-layer (SOL) region, which includes plasma outside the separatrix. Transport properties in this region (which actually will not be discussed in this paper) are dominated by fast longitudinal transport and by atomic physics processes (CX losses, penetration of cold neutrals and impurities). From the point of view of the plasma core, the SOL controls plasma parameters at the separatrix, which play an important role in determining edge MHD stability (both ballooning and kink). Penetration of cold neutrals through the separatrix contributes to edge heat losses and controls particle fuelling in the outer part of plasma volume.

The Edge Transport Barrier (ETB) is a narrow region just inside separatrix, with significantly reduced level of plasma microturbulence. As a result, this region develops strong pressure gradient and large bootstrap currents, which lead to repetitive MHD instabilities (of ballooning, peeling or kink type), so called Edge Localised Modes (ELMs) (see [17] for references). As we discussed earlier, MHD stability is partly controlled by plasma parameters at the separatrix and is therefore linked with the SOL plasma. On the other hand, MHD stability together with the mechanism(s), which control the ETB width, determines plasma parameters on the top of the ETB and provides a link with the plasma core.

Usually a narrow region ($0.8 \leq \rho \leq 0.95$) of not very hot, collisional plasma separates ETB from the plasma core. ELMs, collisional turbulence and cold neutrals dominate transport in this "intermediate" region, which links core with the edge.

Deeper inside (between $0.4 \leq \rho \leq 0.8$) a wide region of quiescent core plasma is positioned, which is usually free of any strong MHD instabilities. The transport is dominated by a drift type of micro-turbulence [1-3], whose main feature is the so called profile stiffness. We will discuss the

concept of profile stiffness in detail later in the paper with only one introductory remark. Profile stiffness suggests that there is a strong link between the core and edge temperature. In other words it means that overall plasma confinement depends on (or is controlled by) the plasma edge. This link between core and edge can be broken by the formation of the Internal Transport Barrier (ITB). An ITB plays a dual role in plasma confinement- on the one hand it breaks profile stiffness and increases plasma performance. On the other hand, it optimises the plasma pressure profile which improves the MHD stability.

Finally, transport in the central part of plasma volume (inside $\rho \leq 0.4$) is either dominated by sawteeth in the conventional scenario or by a region with reduced anomalous transport in discharges with the ITB. Later on we will discuss transport in all enumerated regions. But even before going into detailed discussion, we can draw one important conclusion. Experimental evidence and theoretical considerations suggest that in terms of plasma parameters and underlying transport properties there is a strong link between all five regions. This means that although it is quite legitimate to study anomalous transport in each region independently, it is vitally important to take all regions into account when doing predictive modelling of future devices.

The paper is organised as following. After some deliberation of the transport properties within the ETB and "intermediate" region (Sections 2 and 3), we will concentrate on a detailed discussion of the core plasma transport properties. This includes separate consideration of ion and electron temperature profile stiffness and particle transport (Sections 4,5 and 6). Finally we will discuss the role of the magnetic configuration in the turbulence suppression (Section 7) before giving the Conclusions.

2. EDGE TRANSPORT BARRIER.

The physical mechanism of the edge transport barrier formation is still under discussion, although it is almost universally accepted that L-H transition is controlled by the strong shear in plasma rotation, induced by the radial electric field [4]. What is less clear however is what kind of micro-turbulence is suppressed during the L-H transition. It is known that ITG turbulence, (considered as a main contributor to anomalous transport in the plasma core [5-11]), is very weak near the separatrix. Many researchers point toward drift Alfven wave [12, 13], or resistive peeling or ballooning mode [14] as main contributors to the edge transport. Formation of the ETB will be discussed elsewhere (see, for example [15]), we will concentrate on the transport properties of the ETB after L-H transition. There are two main contributors to that transport. One is a very strong transient transport during the ELM induced by the MHD, and the second one is a reduced transport between ELMs. Experiment shows [16,17] that, as a rule of thumb, integrated energy losses between ELMs is comparable to the losses during the ELMs in type I ELMy H-mode. This excludes, of course, any stationary ELM-free H-modes, observed recently on many tokamaks [18-20], where MHD induced transport contributes very little in terms of heat losses.

We will not discuss here MHD-related transport during the ELMs. Theoreticians are still considering the nature of the MHD instability, which triggers type I ELM- is it a ballooning, peeling or kink mode [17, 21]. Little is known about the non-linear stage of these instabilities either. Recent experiments show [22] that heat and particle losses during the ELM are localised initially in the outer midplane part of the ETB region, which corresponds to a ballooning character of the turbulence. However important is the non-uniformity of particle and heat fluxes during the ELM, this is MHD-related area and it should be discussed elsewhere. We will concentrate on issues related to microturbulence-induced transport and there are two of them to address. The first one relates to time average heat and particle losses in ELMy H-mode plasmas. These losses are actually controlled by the core transport well inside the ETB. The reason is that although ELMs are responsible for any energy and particle edge localised losses, it is core transport, which restores edge energy and particle content between ELMs. This actually allows those who do predictive modelling to use the top of the ETB as an outer boundary for the modelling. Plasma parameters at this boundary are usually selected in accordance with either ballooning or peeling mode stability limit. One should remember however, that both stability limits depend on the pressure and current profiles within the ETB. It is therefore important to include the ETB into the modelling domain with the appropriate transport coefficients in it. Again, there is not much known about transport within ETB between ELMs. The best guess would be to assume that anomalous transport is suppressed completely within the ETB and the only one remaining channel of heat losses is the neoclassical transport. This assumption has been used in [23] in order to find the conditions, under which ELM-free H-mode could become stationary. According to a very simple estimation, the heat flux through the separatrix scales as

$$\text{scales as } q \propto -S \cdot \chi^{i}_{neo} \cdot \nabla n_i T_i \qquad (1)$$

Where S is the separatrix area and χ^{i}_{neo} is ion neo-classical thermal conductivity. In order not to trigger an ELM (which we assume is controlled by a ballooning mode) the pressure gradient within ETB should not exceed ballooning stability limit

$$-\frac{4R \cdot q^2}{B_\phi^2} \cdot \nabla nT \le \alpha_{crit} \qquad (2)$$

Substituting (2) into (1) we get the following estimation for the maximum heat flux through the quiescent neo-classical ETB:

$$Q_{\max} \le 0.25 \cdot S \cdot \chi^{i}_{neo} \cdot \frac{\alpha_{crit} \cdot B_\phi^2}{R \cdot q^2} \propto \alpha_{crit} \cdot \frac{n_{ETB} \cdot Z_{eff}}{\sqrt{T_{ETB}}} \qquad (3)$$

where quantities with subscript ETB mean plasma parameters on the top of the edge barrier. Numerical simulation shows [23] that JET plasmas with reasonably high density and high triangularity can indeed reach a steady state quiescent H-mode. Similar estimations can be done in the case if peeling mode is considered as a main type-I ELM trigger.

3. INTERMEDIATE REGION

The intermediate region is just inside the ETB and its extent toward plasma core is limited by the penetration of cold neutrals and by the extent of ELMs. Usually in a type-I ELMy H-mode it spans from $\rho \leq 0.95$ to $\rho \infty 0.8$. Transport in this region is influenced by ELMs, by atomic physics (CX losses, radiative cooling) and by resistive micro-turbulence (resistive drift ballooning and drift Alfven waves). Despite the universally accepted fact that the intermediate region influences or even controls core transport and overall confinement (see next Sections), transport properties in this region are not well known. As a result, many theoreticians simply impose boundary conditions just inside the intermediate region (at $\rho \cup 0.8$) when doing predictive modelling. This is a reasonable choice in the case when the modelling is aimed on the validation of a particular transport model. The predictive capability of such an approach is, however quite questionable. Another approach is to use either an adapted theoretical transport model (collisional drift ballooning mode [12] in the Multi-Mode transport model (MMM-95) [13]), or an empirical transport model (Bohm coefficient in JET model [24]). Good progress is being made in systematic numerical modelling of transport, generated by the drift Alfven wave turbulence and in parameterisation of this transport as a function of dimensionless plasma parameters [13, 25]. It is worth noting here some previous attempts by a number of theoreticians [26-29]. Clearly any extra efforts in establishing theory based transport model for the edge plasma should be encouraged.

4. CORE CONFINEMENT AND PROFILE STIFFNESS.

The plasma core (confinement region) occupies a wide area between $0.4 \leq \rho \leq 0.8$. It borders on intermediate region from the outside and it is limited by sawtoothing region from inside for conventional scenarios. This region can be divided by an Internal Transport Barrier (ITB). Usually, this re˜ion is free of large scale MHD and therefore its transport is dominated by the microturbulence of a drift type. This region is the best studied both experimentally and theoretically. And profile stiffness (sometime called as profile resilience) is the best known effect, observed in many experiments. Namely, it was observed that ion, and sometimes electron temperature changes in a self-similar way in the core region, so that $T_i(\rho) \propto T_i(\rho = 0.8)$ [30-33]. Figure 2 shows, as an example, the dependence of the core ion temperature as a function of edge temperature for a series of ELMy H-mode ASDEX-Upgrade discharges with different power, density and current. The link between core and edge is clear.

Theoretically self-similarity can be explained by the fact that drift turbulence (Ion Temperature Gradient (ITG), Trapped Electron Mode (TEM) and Electron Temperature Gradient (ETG) mode become unstable only if the relevant relative temperature gradient exceeds some critical level: $\left|\frac{\nabla T}{T}\right| \geq \left|\frac{\nabla T}{T}\right|_{crit}$ In terms of transport this inequality can be re-written in the following form:

$$\chi_i^{ITG} = C \cdot \rho_i^2 \cdot \frac{V_{th,i} \cdot a}{R} \cdot \left(\left|\frac{\nabla T_i}{T_i}\right| - \left|\frac{\nabla T_i}{T_i}\right|_{crit} \right) \qquad (4)$$

where factor in front of the bracket reflects a widely accepted paradigm that drift wave turbulence generates a gyroBohm type of transport. The easiest way to demonstrate the principle of profile stiffness is to assume that fully developed turbulence generates overwhelmingly strong transport, so that:

$$q \approx -S \cdot C \cdot \rho_i^2 \cdot \frac{V_{th,i} \cdot a}{R} \left| \frac{\nabla T_i}{T_i} \right| \cdot n \cdot \nabla T_i >> P \tag{5}$$

where P is the heating power, S is the area of the corresponding flux surface and q is the heat flux. The only one solution for the energy balance equation in this case is to have a temperature profile close to a critical one, so that:

$$\left| \frac{\nabla T_i}{T_i} \right| \approx \left| \frac{\nabla T_i}{T_i} \right|_{crit}, \text{ or } \; T_i(r) \approx T_i(a) \cdot \exp \int_r^a dr \left| \frac{\nabla T_i}{T_i} \right|_{crit} \tag{6}$$

Equivalently, we can conclude that global energy confinement time, defined as $\tau_E \approx \frac{\int dV \cdot (n_e T_e + n_i T_i)}{P} \propto \frac{T(a)}{P}$ does not depend on the core transport in this case. Instead it depends on the transport in the intermediate and edge regions.

In not so extreme cases of finite transport the confinement time does depend on the level of profile stiffness and its study becomes vitally important, particularly when we try to extrapolate our knowledge toward tokamak power plant.

Later on we will discuss ion, electron and particle transport separately. However, before going into detailed discussion, it is worth considering one more general issue of the drift wave turbulence. It follows from the theory (see, for example [1]) that there are three main contributors to electrostatic drift type of turbulence- Ion Temperature Gradient (ITG), Trapped Electron (TEM) and Electron Temperature Gradient (ETG) modes. Generally speaking, these modes have different thresholds. In the case of relatively flat density one can get:

$$L_{Ti}^{crit} \equiv \left| \frac{T_i}{\nabla T_i} \right|_{crit} \approx R \cdot \frac{9}{20} \cdot \frac{T_e}{T_i} \tag{7}$$

for the ITG [1, 5, 6],

$$L_{Te}^{crit} \approx R \cdot \frac{9}{20} \cdot \frac{f_t}{1 - f_t} \tag{8}$$

for the TEM ([2, 34]) with f_t being fraction of a trapped particle and

$$L_{Te}^{crit} \approx R \cdot \frac{1}{(1.33 + 1.88 \cdot \frac{|s|}{q})(1 + Z_{eff} \cdot \frac{T_e}{T_i})} \tag{9}$$

for the ETG mode [35]. In fact, formula (9) is the generalisation of the previously obtained analytical formula for the ITG turbulence [5,6] onto electron branch of the temperature gradient mode. An apparent difference between (7) and (9) is partly attributed to the fact that formula (7) and (9) are

derived under slightly different assumptions. Keeping in mind that each branch of the turbulence generates electron and ion transport as well as particle diffusion and a pinch, we can conclude that profile stiffness is a very complicated concept. In other words it is not easy to find a situation where both electron and ion temperatures stay close to their respective critical marginality throughout the plasma core.

5. ION HEAT TRANSPORT.

Ion heat transport and associated ion temperature profile stiffness is probably the best-studied transport process. Practically all tokamaks observe ion temperature profile stiffness [30-33]. As an example, Figure 3 shows ion temperature profiles (on a logarithmic scale) for a series of JET plasmas with different edge density [32]. One can observe an obvious self-similarity of the core ion temperature (from $R \infty 3.3m$ R to $R \leq 3.7m$). Another example come from recent experiment on JT-60U, where gas puffing and Ar seeding have been used to modify edge ion temperature [33]. As it follows from Figure 4, JT-60U also observes ion temperature profile stiffness within $0.4 \leq \rho \leq 0.85$. Interestingly the observed level of profile stiffness seems to depend on machine size- smaller tokamaks report a higher level of profile stiffness than larger tokamaks. The higher level of specific heating power, achieved in smaller tokamaks together with the relatively weaker electron-ion equipartition might explain this trend.

It is worth noting that there is no complete consensus yet about the level of expected profile stiffness even between theoreticians. Several groups of theoreticians have published recently the result of their joint research on the level of profile stiffness, induced by the ITG mode [36]. Briefly the result is summarised in Figure 5, where the normalised ion thermal conductivity as a function of the departure from the critical temperature gradient is shown for a series of non-linear numerical simulations of the ITG turbulence, made by different groups. One can observe that, in general, gyro-fluid codes generate visibly stronger transport than those codes, which use gyro-kinetic or quasi-linear approximations. The observed difference is the result of the extreme complexity of the problem and theoreticians are still investigating it. Here we'll just give some illustration on how advanced and complicated is the modern theory of anomalous transport by using the observed non-locality of plasma turbulence as an example. The main experimental observation of plasma turbulence non-locality is usually associated with the fast propagation of a temperature perturbation induced by local changes of the temperature near plasma edge [37,38]. Originally it was suggested that the non-locality could be explained by the long radially correlated turbulence vortices, generated either by the non-linear inverse cascading or by toroidal mode coupling. It was even proposed that such long correlated turbulence might be responsible for the experimentally observed Bohm-type of confinement in the L-mode plasma. However, numerical simulations of the drift type of plasma turbulence have shown [39] that these long correlated structures are usually destroyed by the self-generated zonal flows during the non-linear phase of the turbulence generation. In this respect an interesting result has been presented recently by Z. Lin et al., [40]. A full torus gyro-kinetic simulation

of the drift turbulence has revealed that indeed the characteristic size of the turbulent vortices does not scale as a machine size (see Figure 6). Therefore one might expect that such turbulence would create gyroBohm type of transport. Surprisingly, recent, preliminary spectral analysis of the very similar simulation [41] showed that this turbulence sometimes generates Bohm-type of anomalous transport. Several explanations have been proposed to resolve the apparent contradiction. One explanation attributes enhanced transport to a finite plasma collisionality. Indeed it was shown [42] that ion-ion collisions can inhibit self-generated zonal flow and therefore increase the level of long radially correlated vortices. The second one attributes an enhanced transport to the fact that self-generated zonal flows as well as long correlated vortices have an intermittent character. The intermittent nature of plasma turbulence has been studied recently both experimentally [43] and theoretically [41, 44]. Both groups use a statistical approach, which decomposes plasma turbulence (or associated turbulent heat flux) into sum over heat fluxes $q_\perp(r,t) \equiv \sum_i q_i(r,t)$ of different sizes h_i, where $h_i \equiv \int d^3\, r dt \cdot q_i(r,t)$. If we define f(h) as a probability distribution function (PDF) of a heat pulse of magnitude h, then $\langle q_\perp \rangle \equiv \frac{1}{V \cdot T} \int_V d^3 r \int_T dt q_\perp(r,t) = \int dh \cdot h \cdot f(h)$. then the crucial question is which value of h contributes most to this integral? Statistical analysis of both experimental observations and theoretical consideration show that generally PDF has some plateau $f(h) \approx f(h_{cr})$ or short scale heat pulses with $h \le h_{cr}$ and a tail of long correlated heat pulses with $f(h) \approx f(h_{cr}) \cdot \left(\frac{h_c}{h} \right)^{\alpha}$ (see Figure 7). Recent analysis of full torus 3-D gyro-kinetic ITG turbulence simulation reveals that such turbulence an generate a tail of long correlated heat pulses with an exponent $\pm < 2$, which lead to Bohm or stochastic transport scaling [41]. It has been shown as well that the exponent $\pm$ increases above $\pm > 2$ (which correspond to gyroBohm transport) in case when a substantial externally induced sheared plasma rotation is applied (compare with L-H transition).

Predictive modelling is one of the commonly used tools to study profile stiffness. Two aspects of profile stiffness are usually discussed in connection with predictive modelling. The first one addresses the issue of the experimentally observed link between core and edge temperature and ability of transport model to reproduce this link. The second one deals with the problem of fast heat pulse propagation [38] and the observation in some experiment of the change in the heat pulse polarity, when negative temperature perturbation near plasma edge get positive in the central part of plasma volume [37]. There are several theory based transport models with the different level of profile stiffness [7-9, 45] and empirical models, which incorporate some kind of profile stiffness [24]. One should remember that due to a difference in the level of profile stiffness even those models, which have very similar physics (same branch of the turbulence included into a model), could generate different transport with different level of profile stiffness. Figure 8 shows a result of a recent test of theory based transport models against previously discussed series of ASDEX-Upgrade plasmas [46]. The authors conclude that all ITG models reproduce experimental data quite well with Weiland model (the one with the weakest profile stiffness) doing marginally better than others. The CDBM

model does not reproduce profile stiffness and underpredicts core ion temperature. Similar conclusion has been recently drawn in [47], where both theory-based and empirical transport models have been tested against JT-60U data with on and off-axis NBI heating (see Figure 9). Both theory-based and empirical transport models with introduced profile stiffness reproduce the experiment quite well.

6. ELECTRON HEAT TRANSPORT.

From the theory point of view electron heat transport is much less studied than its ion counterpart for two main reasons. Firstly, electron transport is much more influenced by electromagnetic turbulence. Secondly, it is more influenced by the short wavelength turbulence with a characteristic perpendicular wavelength of the order of electron Larmor radius. Both these factors make numerical simulation much more complicated. On the other hand, experimentally electron transport is relatively well studied thanks to easily available Electron Cyclotron Emission (ECE) measurements of the electron temperature, with very good time and space resolution. One important condition for successful study of electron transport is an ability to separate electron and ion heat fluxes so that the ion-electron heat exchange (which is difficult to quantify in cases with relatively high density and $\left|T_e - T_i\right| \Big/ T_e \ll 1$ would play only minor role. This is easy to do in discharges with relatively low density and pure electron heating (with ECRH and some scheme of ICRH). Cold pulse, triggered by laser ablation, is a valuable tool to study transient electron transport as well. There is one more limitation, which influences our ability to study electron transport in general and electron temperature profile stiffness in particular. The problem is that all three branches of drift turbulence under discussion- ITG, TEM and ETG modes generate both electron and ion transport. And, as a rule of thumb, $\chi_\perp \propto \frac{\gamma}{k_\perp^2} \propto k_\perp^{-1}$ and transport coefficients are mainly controlled by the turbulence with the longest wavelength. For the above-mentioned modes the ITG turbulence has the longest wavelength and therefore it should dominate transport, if excited. And, as follows from (7), its destabilisation is mainly controlled by the relative ion temperature gradient (although $L_{Ti}^{crit} \propto \frac{T_e}{T_i}$ does depend on electron temperature). Therefore, to study electron temperature profile stiffness, one should try to minimise the role of ITG in first place. Since $L_{Ti}^{crit} \propto \frac{T_e}{T_i}$ and $\gamma_{ITG}, \propto \frac{1}{L_{Ti}} - \frac{1}{L_{Ti}^{crit}}$ pure electron heating can actually destabilise ITG. The advantage of pure electron heating combined with low density is that the heat flux, which is transmitted through ion channel, is minimal in this case. This should keep ITG mode very close to its marginal stability so that other instabilities with shorter wavelength start to play dominant role.

Electron transport and the associated electron temperature profile stiffness have been thoroughly reviewed in [48]. A number of tokamaks observed stiffness in electron temperature profile in plasmas with ECRH heating; some examples are shown on Figure 10.

As discussed earlier, Fast Waves in Ion Cyclotron Resonance range of frequencies can provide direct electron heating. Such scheme has been recently utilised in Tore Supra to study electron

transport [49]. Figure 11 compares the experimentally observed electron temperature gradient length L_{Te} with the critical temperature gradient for the ETG turbulence from [35]. The authors conclude that the dependence of the critical temperature gradient scales agrees with the theory of ETG. However the fact that the value of observed R/L_{Te} systematically exceeds theoretical value indicates that either theoretical approximation used in (9) is not adequate, or that ETG induced transport is week and there are other instability in force (TEM or ITG) to ensure profile stiffness.

It is worth noting that not all tokamaks observe strong stiffness of electron temperature, and even those who do observe it, report that the level of profile stiffness depends on the edge temperature [48]. Partly this can be attributed to the fact that sometimes it is difficult to separate electron and ion heat losses. In other experiments electron transport might be controlled by two or more instabilities simultaneously (and also by electromagnetic effects, which are missing in present studies). High k fluctuation measurements on TFTR have shown [50] that these fluctuations propagate in the ion diamagnetic direction (contrary to the ETG theory predictions). Predictive modelling provides a good indication on the complexity of electron temperature stiffness. Figure 12 shows the result of recent test of different theory based transport models against ASDEX-Upgrade data for electron heating [46]. Interestingly, the best agreement with experiment has been achieved by using Weiland model, which does not include ETG-related transport.

Theoretically, a lot of efforts has been recently devoted to a detailed simulation of short wavelength ETG turbulence [51]. Previously theoreticians were sceptical about the possible role of the ETG turbulence in electron transport. The source of this scepticism lies in the fact that this instability generates turbulence with a very short wavelength of the order of electron Larmor radius. In accordance with above-mentioned rule of thumb $\chi_\perp \propto k_\perp^{-1}$ which makes ETG insignificant in terms of transport. Two factors have led to a reconsideration of the role, that the ETG turbulence can play in electron transport. The first one is associated with the growing popularity of plasmas with Internal Transport Barrier (ITB). To explain it, we will once again use the rule of thumb argument. It is universally accepted that the ITB formation is generally controlled by the strong shear in plasma rotation [4], so that the turbulence is stabilised when the shearing rate $\omega_{E\leftarrow B}$ exceeds maximum growthrate γ_k^{max} of unstable mode. Since shearing rate $\omega_{E\leftarrow B}$ does not depend on the wavelength of the turbulence and $\gamma_k^{max} \propto k_\perp^{max}$ one can conclude that it should be much easier to suppress long wavelength branches like ITG or even TEM, but it would be extremely difficult to get rid of the ETG turbulence by conventional means. This makes ETG responsible for an observed finite electron transport in plasmas with ITB. The second factor, which makes the ETG model meaningful from a transport point of view is non-linear advection, or non-linear inverse cascading of unstable waves into the longer wavelength part of a spectrum. This process is not very effective in case of the ITG because of the damping, induced by the self-generating shearing flow (see above). Recent detailed numerical simulation of ETG turbulence reveals that, unlike its ITG counterpart, ETG generates relatively long radially correlated vortices, which are not destroyed by the self-generated flow [51,52] (see Figure 13). This has been explained by the fact that sheared plasma rotation influence very weakly turbulence with wavelength shorter than the characteristic ion Larmor radius [51,52].

If ETG turbulence can not (at least practically) be suppressed by shear in plasma rotation, is there any other way to influence it? Partly this question was addressed in above-mentioned simulations of the ETG turbulence, although described in these papers mechanism of so called s-± stabilisation has actually a very long history [53,54]. Figure 14 shows an example of s-± stabilisation of the ETG turbulence from a recent non-linear simulation [52]. The shaded area with circles indicates the region with strong transport. We can draw a conclusion that the negative magnetic shear reduces the level of the ETG turbulence (as well as some other instabilities).

We suggested from the very beginning that we would not discuss physics of the edge or core transport barrier formation and its dynamics. However, since we already mentioned the role of a negative shear in the turbulence stabilisation, to balance the argument we briefly enumerate some other ways in which magnetic configuration can influence anomalous transport.

First, it was shown both analytically and in non-linear numerical simulations [56] that a region with zero magnetic shear separates vortices (particularly those with long correlation length) thus reducing transport.

Secondly, a region with small or zero magnetic shear has a less dense population of rational surfaces, around which turbulent vortices are usually localised [57]. Therefore, once again, we might expect the anomalous transport be somehow reduced near zero magnetic shear. For the sake of argument it is worth mentioning here that some theoreticians challenge this second mechanism, saying that this "trimming" of the rational surfaces near zero shear is valid for low m and n numbers only. Short wavelength turbulence should not be influenced by the proximity of zero magnetic shear. In any case, it is widely accepted that anomalous transport might be significantly reduced if zero magnetic shear coincides with low m and n integer or simple rational magnetic surface, like q=2. Indeed many experiments indicate that it's much easier to form an ITB if the region with small magnetic shear contains the q=2 surface.

The role of integer or simple rational magnetic surfaces in a formation of electron transport barriers has been discovered and carefully investigated on RTP [58] (and later on many other tokamaks [59]). Figure 15 shows a well known example from RTP, in which the position of the ITBs has been studied by an accurate measurement of electron temperature profile variation due to a series of carefully crafted shifts in the position of EC resonance. Electron temperature drops or jumps as soon as the ECR heating zone crosses the position of the nearest low order rational magnetic surface. The RTP result has been recently reproduced in non-linear numerical simulations of global, two fluids, long wavelength electromagnetic turbulence [60]. The simulations capture features associated with the formation of the ITBs, and qualitatively reproduce some of the observations made on RTP. The role of electromagnetic effects and those of induced radial electric field play important role in the non-linear dynamics of the turbulence. Figure 16 confirms qualitative agreement between modelling and observation on RTP.

Finally a few words about transient phenomena- probably one of the most powerful and challenging methods to study transport. This method includes all types of cold and heat pulses,

triggered at the plasma edge (laser ablation, L-H-L transitions) as well as core heat pulses (localised heating, ITB formation). The method is particularly valuable for those who study electron transport, first of all because of widely available ECE diagnostics with very good time and space resolution. The method is also known as a major contributor toward long lasting discussion on the non-locality of plasma turbulence [37,38]. We mention here only some recent results on the modelling of the heat pulses [61,62], where the authors tested different theory based transport models against a wide range of transient phenomena, including reheating of the plasma core in TEXT [37]. The diversity of experimental situations makes it very difficult to draw any universal conclusion about these modelling activity. Tentatively we conclude that those heat pulses, which are initiated deep in the plasma core, do not show any sign of non-locality and therefore do not require strong electron temperature profile stiffness to get an agreement with experiment [62]. Cold pulses, which are triggered near plasma edge, often result in a very fast inward propagation (sometimesaccompanied by the reheating of the core). Analysis shows that strong profile resilience is required to explain these phenomena [61].

Recently the cold pulse technique has been used in JET Optimised Shear plasmas. The idea was to see how the cold pulse propagates through the ITB [63]. Figure 17 shows time evolution of the temperature perturbation, caused by such a cold pulse. The authors conclude that the cold pulse (CP) progressively erodes the outer ITB portion. The ITB foot moves inward by ~ 4 cm. This generates a large CP. The inner ITB portion however acts to strongly damp the CP so that it vanishes in the core region. The experimental observations have been reproduced with an empirical transport model which assumes that transport in the ITB is mainly diffusive and non-stiff, no heat pinch required.

6. PARTICLE TRANSPORT.

Anomalous particle diffusion and pinch are the least studied transport properties, both theoretically and experimentally. The theoretical investigation of particle transport is complicated by the problem of ambipolarity, which means that particle diffusion is controlled by the least mobile component, usually electrons. The study of electron transport itself is rather complicated, since it involves short wavelength turbulence and includes electromagnetic effects. As a result the only available theory based transport model for ambipolar particle transport is one, which uses a quasi-linear approximation [7]. Experimentally investigation of particle transport is also complicated by at least three factors. First of all, it requires time dependent measurements in order to distinguish between anomalous diffusion and pinch. This, in turn, requires diagnostics with good enough time and space resolution, which are not easily available. On the top of that, the density profile is in many cases influenced by the cold recycled neutrals, whose distribution is poloidally asymmetrical and therefore very difficult to measure or calculate. As a result, we can draw only tentative conclusions and limit our consideration by two issues, which are of the greatest importance for the future tokamak-reactor.

The first one is experimentally observed degradation of plasma confinement while plasma approaches density limit [64,65]. This phenomenon has been observed in practically all tokamaks;

Figure 18 shows, as an example, a recent result from JET [66], which demonstrates that confinement degradation can be shifted towards higher density by an increase in plasma triangularity. The following explanation has been proposed to explain observed phenomenon. Usually (see later) strong gas puffing is required in ELMy H-modes in order to increase the plasma density above its "natural" level. As a result, the edge density rises faster than the central density so that the density profile becomes flatter. Next we will assume that plasma pressure on the top of edge transport barrier is controlled by the ballooning stability, so that , $\frac{4R \cdot q^2}{B_\phi^2} \cdot \frac{n_B T_B}{\Delta} \le \alpha_{crit}$ where Δ is the ETB width and n_B and T_B are respectively plasma density and temperature on the top of the barrier. It follows from the ballooning stability that, even if the transport barrier width does not change, the edge temperature scales inversely to the edge density. Now if we take into account profile stiffness, we find that core temperature should drop in proportion to edge temperature. Taken together with the density profile flattening, this results in confinement degradation. Numerical simulation shows however [67], that in order to get reasonable agreement with the experiment above mentioned mechanism should be combined with an assumption that transport barrier width shrinks with the edge density. This assumption is in line with some theoretical models [68], which predict that edge transport barrier width scales with thermal ion Larmor radius. Finally, if gas puffing exceeds a certain level, the edge transport barrier collapses and plasma returns to L-mode.The second issue, which is directly related to a tokamak power plant, is the question of the existence of an anomalous pinch. The pinch effect (usually inward directed for particle transport) theoretically is a well-known phenomenon (see, for example, [69-71]). As mentioned above, an inward pinch is automatically included into transport model deduced from the quasi-linear theory [7], although in practice it might be not an easy task to separate it. Experimental observations of an anomalous inward pinch are very incomplete, and sometimes even contradictory. We have already mentioned several problems, which complicate experimental observation of anomalous pinch. On the top of that, many experiments indicate that an anomalous pinch, if it exists, is localised in the outer part of plasma volume [71]. The density profile in this region is influenced by cold neutrals, which complicate the analysis even more. To demonstrate the complexity of analysis it is illuminating to look at recent experimental attempts to increase plasma density above Greenwald limit by using slow gas puffing together with NBI fuelling. Such an experiment was first conducted on DIII-D [72] and repeated later on JET and ASDEX-Upgrade. Some characteristic time traces of DIII-D high-density plasma and density profile evolution during slow gas puff are shown in Figures 19 and 20. Experiments have revealed that immediately after the application of gas puff the edge density increases relative to the core (and this is accompanied by a noticeable degradation in plasma confinement). As the density wave moves inward, the profile becomes peaked. During this stage, the energy content increases monotonically, and eventually exceeds its initial value.

Similar results were recently reported by JET team [73] with the main conclusion that a combination of a slow gas puffing and NBI fuelling indeed allows the raising of the electron density

above Greenwald limit without degrading confinement. Figure 21 shows the target density profile in the beginning of slow gas puffing and density profile during the advanced stage of the density rise. An attempt has been made recently [74] to reproduce experimental results by using predictive modelling. Two transport models have been used to simulate the JET result shown in Figure 21. The first one was the empirical JETTO Bohm/gyroBohm model with neo-classical Ware pinch only. The other was theory based Weiland model, which includes off-diagonal elements with the self-consistent anomalous pinch. Figure 22 compares measured electron density profile just before radiative collapse with the simulated density profiles. First of all one can conclude that Weiland model (the one with anomalous pinch) reproduces density peaking visibly better than the model without the anomalous pinch. Secondly we can say that the Weiland model slightly overestimate the central density (or one can say that it underestimates transport near plasma centre). Having said that, it is worth noting that such good agreement between experiment and Weiland model does not come easily. To begin with, it was necessary to remove the density flattening by sawteeth (which apparently happened in experiment as well). After that density starts to get peaked mainly due to beam fuelling. At a certain stage the density peakedness exceeds some critical level so that ITG turbulence is stabilised in the central part of plasma volume. After that the central density simply follows beam fuelling. It does not mean that anomalous pinch does not play any role in this experiment. Anomalous pinch is important, but it influences the outer half of plasma volume only.

7. SUMMARY

Heat and particle transport in the tokamak is one of the most challenging areas in plasma physics. Its complexity is being reconsidered recently since the realisation of the fact that the edge and core plasma are linked together by profile stiffness. Recognition of this fact has changed dramatically our assessment of the predictive capability of our codes and scaling laws. If previously we could easily ignore a narrow edge region, which is usually influenced by atomic physics processes, saying that since it is very thin and so its contribution to overall energy content is negligible, now we should consider it because of the link between core and edge transport.

There are some ways to break the link between core and edge by triggering either edge or internal transport barriers, or both. However one can look at this problem from the different angle. Namely by introducing transport barriers we are just bringing in new physics into consideration by bridging edge and core plasmas with the layers, which have different transport characteristics. One can say that the formation of transport barriers makes the coupling between “inside” and “outside” plasmas looser but the link still exists.

The concept of profile stiffness has been studied both theoretically and experimentally for a number of years. It is fair to say that the core ion heat transport is the best-studied component of anomalous transport. It is controlled by the long wavelength turbulence, which is the easiest for both non-linear numerical simulations and for experimental investigation. A number of theory based transport models have been elaborated during the past few years and they have been rigorously tested in

predictive numerical modelling. Generally models, which are based on ITG and TEM turbulence, reproduce ion heat transport reasonably good. The level of profile stiffness is, however, still under discussion.

Electron heat transport is probably one of the most active areas of recent research. Theoretically it is much more complex than ion transport due to the shorter wavelength turbulence involved and possible role of electromagnetic effects. Experimentally good progress has been achieved by using scenarios with pure electron heating, such as ECR or Fast Wave heating schemes. Theoretical activity now concentrates on two main issues:
a) Electromagnetic turbulence (with a relatively long wavelength), which ought to explain the observed transport barrier formation close to low order rational or integer magnetic surfaces. b) Very short wavelength ETG turbulence, which, due to inverse non-linear cascading, might be responsible for an observed finite electron transport inside ITB.

The study of the turbulence non-locality remains a very active area of both experimental and theoretical research. This involves measurements of the turbulence PDF, particularly of a long-correlated tail of the distribution function. A lot of theoretical activity centres around the so called full torus non-linear modelling of plasma turbulence in tokamak. This is aimed on studying of the long correlated vortices and turbulence intermittence in a real tokamak geometry, including region with zero and negative magnetic shear.

Particle diffusion and the pinch effect are the least studied part of anomalous transport. The experimental study is complicated by the scarcity of high-resolution diagnostics and by the influence of cold neutrals, recycled from the wall, which complicate study of particle transport in the outer part of plasma volume. Theoretically restrictions, imposed by ambipolarity, complicate dramatically the non-linear numerical simulations of particle transport and put its practical realisation very difficult to achieve. On the other hand the quasi-linear approach, used by some theoreticians, does give valuable information about particle transport and the anomalous pinch, which is being used in predictive modelling. Some comparison with experiment has been done, with more progress expected in the future.

8. ACKNOWLEDGEMENTS

This work has been performed under the European Fusion Development Agreement and was funded by Euratom and the UK Department of Trade and Industry.
The author would like to thank the following people for providing material for this paper: T. Fukuda, L. Garzotti, G.T. Hoang, W. Horton, F. Jenko, Z. Lin, M.A. Mahdavi, P. Mantica, D.R. Mikkelsen, W. Nevins, F. Ryter, G. Saibene, J. Stober, T. Tala, G. Tardini, A. Thyagaraja, H. Urano, M. Valovi , J. Weiland.

REFERENCES

[1] J. Weiland, in†"Collective Modes in Inhomogeneous Plasma, Institute of Physics Publishing, Bristol and Philadelphia, 2000;

[2] X. Garbet, in Proceedings of the 28th EPS Conference on Controlled Fusion and Plasma Physics, Madeira, Portugal, 2001;

[3] 3. W. Horton, B.-G. Hong and W.M. Tang, Phys. Fluids, **31**, 2971 (1988);

[4] T.S. Hahm and K.H. Burrell, Phys. Plasmas **2**, 1648 (1995);

[5] F. Romanelli, Phys. Fluids B1, 1018 (1989);

[6] T.S. Hahm and W.M. Tang, Phys. Fluids B1, 1185 (1989);

[7] H. Nordman, J. Weiland, A. Jarmen, Nuclear Fusion **30**, 983 (1990);

[8] M. Kotschenreuther, W. Dorland et al., Phys. Plasmas, **2**, 2381 (1995);

[9] 7. R.E. Waltz et al., Phys. Plasmas, **4**, 2482 (1997);

[10] A.J. Redd, A.H. Kritz, G. Bateman and J. Kinsey, Phys. Plasmas **4**, 2207 (1997);

[11] D.R. Mikkelsen et al., in Proc. 17th Fusion Energy Conf., Yokohama, Japan, 1998, CN-69/ ITERP1/08;

[12] P.N. Guzdar, J.F. Drake, D. McCarthy et al., Phys. Fluids, **B5**, 3712 (1993);

[13] G. Bateman, A.H. Kritz, A.J. Redd et al., in Proc. of 17th IAEA Fusion Energy Conf., Yokohama, Japan, 1998, IAEA-F1-CN-69/THP-2-19;

[14] H.R. Wilson, J.W. Connor, A.R. Field et al., ibid. CN-69/TH3/3;

[15] P. Gohil, this issue;

[16] G.M. Fishpool, Nucl. Fusion, **38**, 1373 (1998);

[17] W. Suttrop, Plasma Phys. Contr. Fusion **42**, Supplement 5A, A1, 2000;

[18] M.J. Greenwald et al., Phys. Plasmas, **6**, 1943 (1999);

[19] E.J. Doyle et al., in Proc. 18th Fusion Energy Conf., Sorrento, Italy, 2000, CN-69/EX-6/2;

[20] M. Becoulet et al., this issue;

[21] 19. A. D. Turnbull et al., ., in Proc. 18th Fusion Energy Conf., Sorrento, Italy, 2000, CN-69/ TH3/6;

[22] N. Oyama et al., this issue;

[23] V. Parail et al, in Proceedings of the 28th EPS Conference on Controlled Fusion and Plasma Physics, Madeira, Portugal, 2001;

[24] M. Erba et al., Plasma Phys. Contr. Fusion, **39**, 261 (1997);

[25] B. Scott, Plasma Phys. Contr. Fusion, **39**, 1635 (1997);

[26] O. Pogutse et al. in Proceedings of the 24th EPS Conference on Controlled Fusion and Plasma Physics, Berchtesgaden, Germany, 1997;

[27] B.D. Scott, Plasma Phys. Contr. Fusion **39**, 471 (1997);

[28] A. Zeiler, J.F. Drake et al., Phys. Plasmas **3**, 2951 (1996);

[29] J.F. Drake aet al., Phys. Rev. Letters **3**, 494 (1995);

[30] J. Stober et al., Plasma Phys. Contr. Fusion, **42**, A211 (2000);

[31]. W. Suttrop et al., Plasma Phys. Contr. Fusion, **39**, 2051 (1997);
[32] L.D. Horton et al., Plasma Phys. Contr. Fusion, **41**, B329 (1999);
[33] H. Urano, this issue;
[34] B.B. Kadomtsev and O.P. Pogutse, Sov. Phys.-Dokl., 14, 470 (1969);
[35] W. Horton et al., Phys. Plasmas, **7**, 1494 (2000);
[36] A.M. Dimits et al., Phys. Plasmas **7**, 969 (2000);
[37] K.W. Gentle et al., Phys Rev. Letters **74**, 3620 (1995);
[38] V.V. Parail et al., Nuclear Fusion, **37**, 481 (1997);
[39] T.S. Hahm et al., Phys. Plasmas 6, 922 (1999);
[40] Z. Lin et al., in Proc. 18th Fusion Energy Conf., Sorrento, Italy, 2000, CN-69/TH-2/3;
[41] W. Nevins et al., APS, 2000;
[42] M.N. Rosenbluth and F.L. Hinton, Phys. Rev. Letters, **80**, 724 (1998);
[43] R. Sanchez, D.E. Newman, B.A. Carreras, in Proc. 18th Fusion Energy Conf., Sorrento, Italy, 2000, CN-69/THP1/08;
[44] D.E. Diamond, B.A. Carreras and P.A. Diamond, Phys. Letters A **218**, 58 (1996);
[45] S.-I. Itoh, K. Itoh et al., Plasma Phys. Contr. Fusion, **38**, 1743 (1996);
[46] G. Tardini et al., Nuclear Fusion **40**, ...(2000);
[47] D.R. Mikkelsen et al., submitted to Nuclear Fusion;
[48] F. Ryter et al., in Proceedings of the 28th EPS Conference on Controlled Fusion and Plasma Physics, Madeira, Portugal, 2001;
[49] G.T. Hoang et al., ibid.;
[50] K.L. Wong et al., Phys. Letters A236, 339 (1997);
[51] F. Jenko et al., Phys. Plasmas, **7**, 1904 (2000);
[52] W. Dorland et al., , in Proc. 18th Fusion Energy Conf., Sorrento, Italy, 2000, CN-69/TH-2/5;
[53] B.B. Kadomtsev, O.P. Pogutse, Sov. Phys. JETP **24**, 1176 (1967);
[54] T.M. Antonsen, Jr., J.F. Drake, P.N. Guzdar, Phys. Plasmas **3**, 2221 (1996);
[55] H. Biglari, P.H. Diamond and P. W. Terry, Phys. Fluids **B2**, 1 (1990);
[56] Y. Kishimoto et al., , in Proc. 17th Fusion Energy Conf., Yokohama, Japan, 1998, CN-69/ TH1/2;
[57] X. Garbet et al., Phys. Plasmas, **6**, 2793 (2001);
[58] G.M.D. Hogeweij et al., Nucl. Fusion **38**, 1881 (1998);
[59] N. Lopes Cardozo et al., Physicalia **20**, 169 (1998);
[60] A. Thyagaraja, Plasma Phys. Contr. Fusion, **42**, B255 (2000);
[61] J.E. Kinsey et al., Phys. Plasmas **6**, 1865 (1998);
[62] G. Tardini et al, in Proceedings of the 28th EPS Conference on Controlled Fusion and Plasma Physics, Madeira, Portugal, 2001;
[63] P. Mantica et al., ibid.;
[64] S. Hugil, in 2nd Joint Varenna-Grenoble Symposium, Brussels, Belgium, 1980, p.775;

[65] M. Greenwald et al., Nucl. Fusion, **28**, 2199 (1988);
[66] G. Saibene et al., , in Proceedings of the 28th EPS Conference on Controlled Fusion and Plasma Physics, Madeira, Portugal, 2001;
[67] V. Parail et al., , in Proceedings of the 27th EPS Conference on Controlled Fusion and Plasma Physics, Budapest, Hungary, 2000;
[68] T. Hatae et al., in Proc. 18th Fusion Energy Conf., Sorrento, Italy, 2000, CN-69/ITERP/03;
[69] R.R. Domingez Phys. Fluids, **B5**, 1782 (1993);
[70] V.V. Yan'kov, J. Nikander, Phys. Plasmas **4**, 2907 (1997);
[71] D.R. Baker, M.N. Rosenbluth, Phys. Plasmas **5**, 2936 (1998);
[72] M.H. Mahdavi et al., in Proc. 18th Fusion Energy Conf., Sorrento, Italy, 2000, CN-69/EXP1/04;
[73] M. Valovic et al., in Proceedings of the 28th EPS Conference on Controlled Fusion and Plasma Physics, Madeira, Portugal, 2001;
[74] V. Parail et al., ibid.;

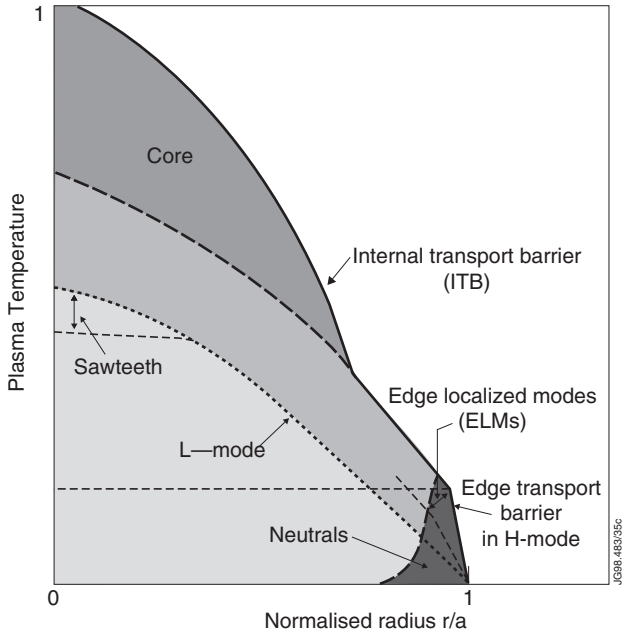

Figure 1. Schematic view showing regions with different transport characteristics in tokamak

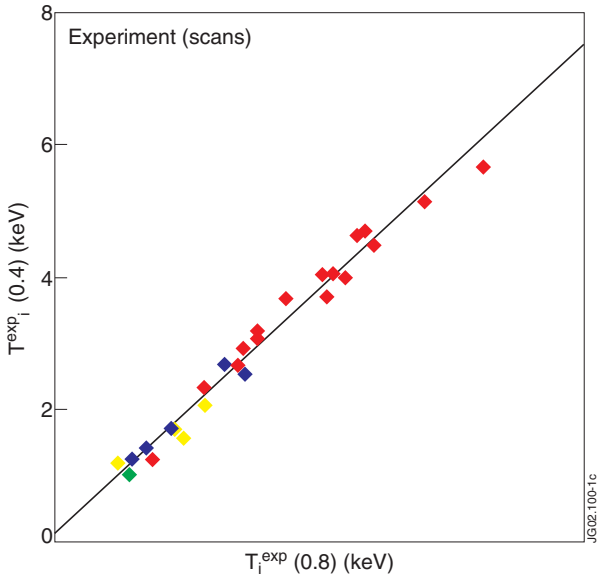

Figure 2. Link between central and edge ion temperature for a series of ASDEX-Upgrade discharges [30]

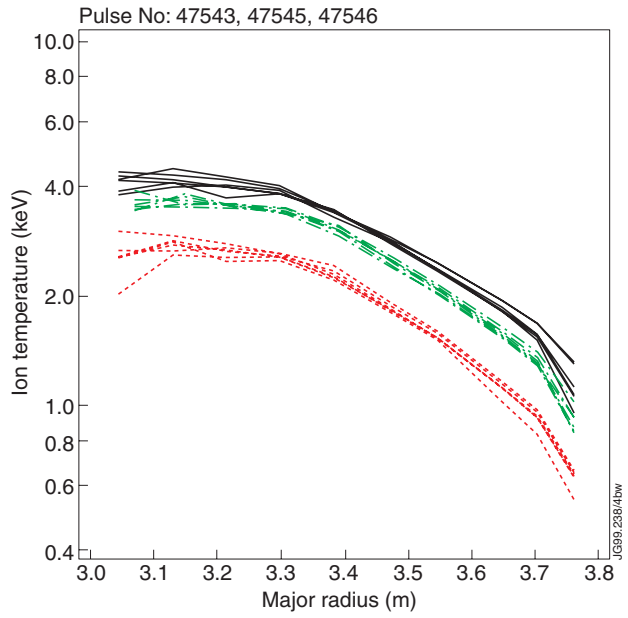

Figure 3.Ion temperature profile for a series of JET shots with varying edge density and edge ion temperature [32].

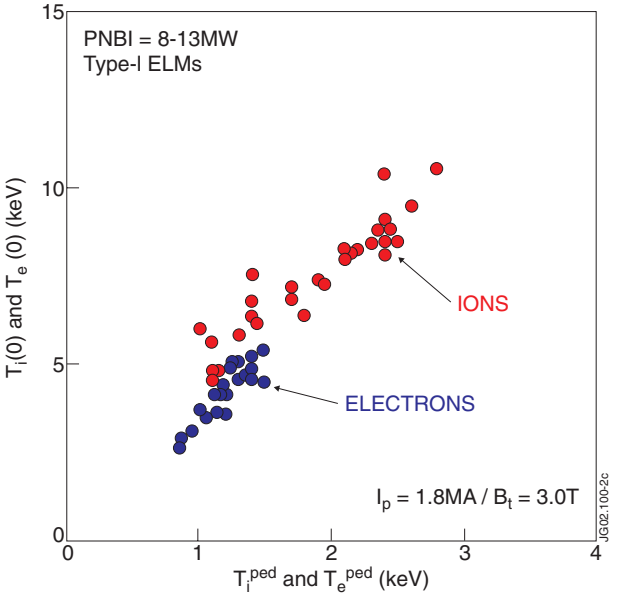

Figure 4.Link between central and edge temperature in a series of JT60-U plasmas [33]

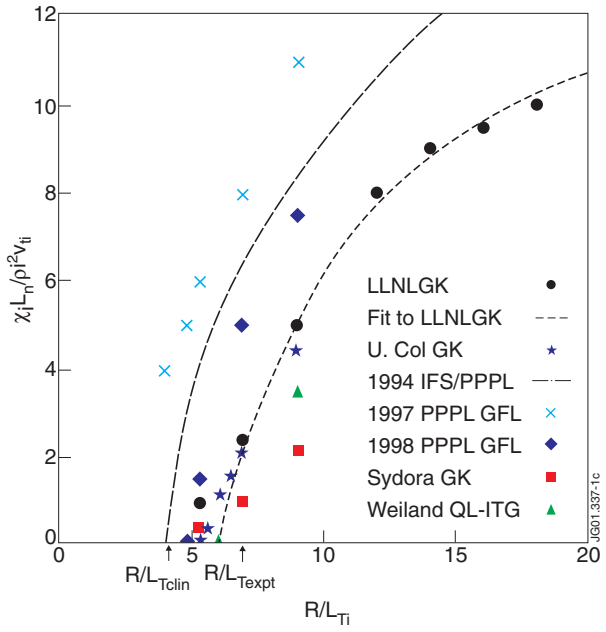

Figure 5. Normalised ion thermal diffusivity as a function of relative temperature gradient, computed for the ITG turbulence by a number of gyro-fluid and gyro-kinetic codes [36].

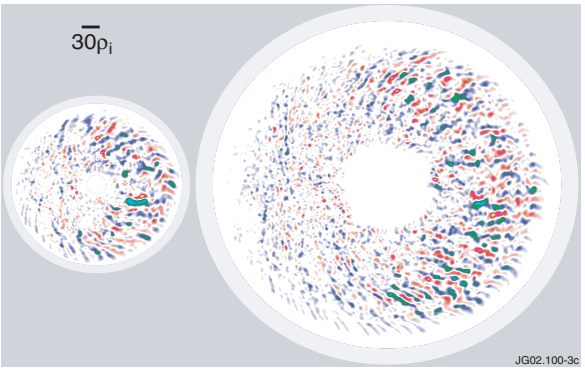

Figure 6. Comparative characteristics of Δ contours for the ITG turbulence in two tokamaks with different size [40]

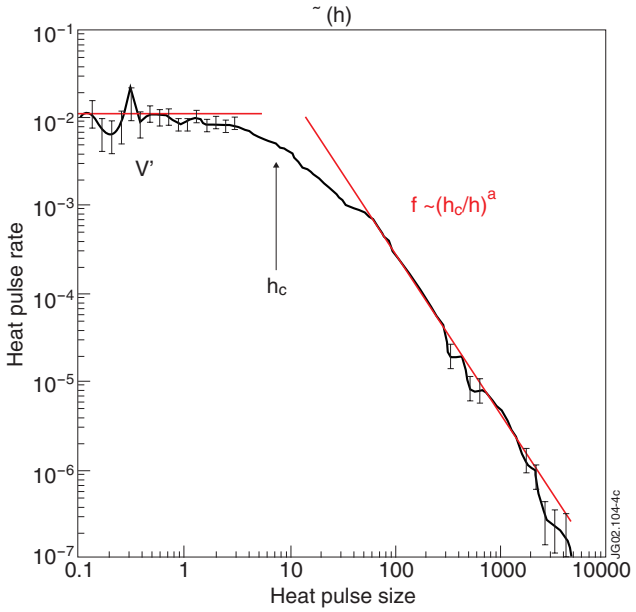

Figure 7. General form of PDF for the turbulence induced heat pulses [41]

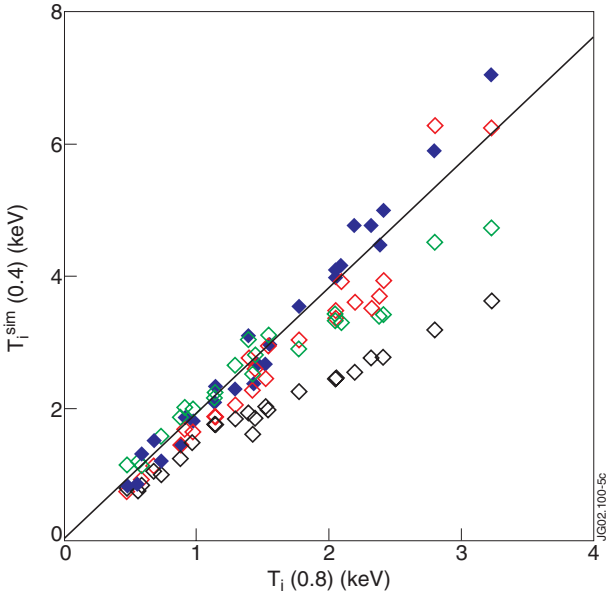

Figure 8. Simulated core and edge temperatures; blue diamonds correspond to Weiland model, green diamonds to GLF23, red to IFS/PPPL and black to CDBM. Line reproduces the experimental points [46].

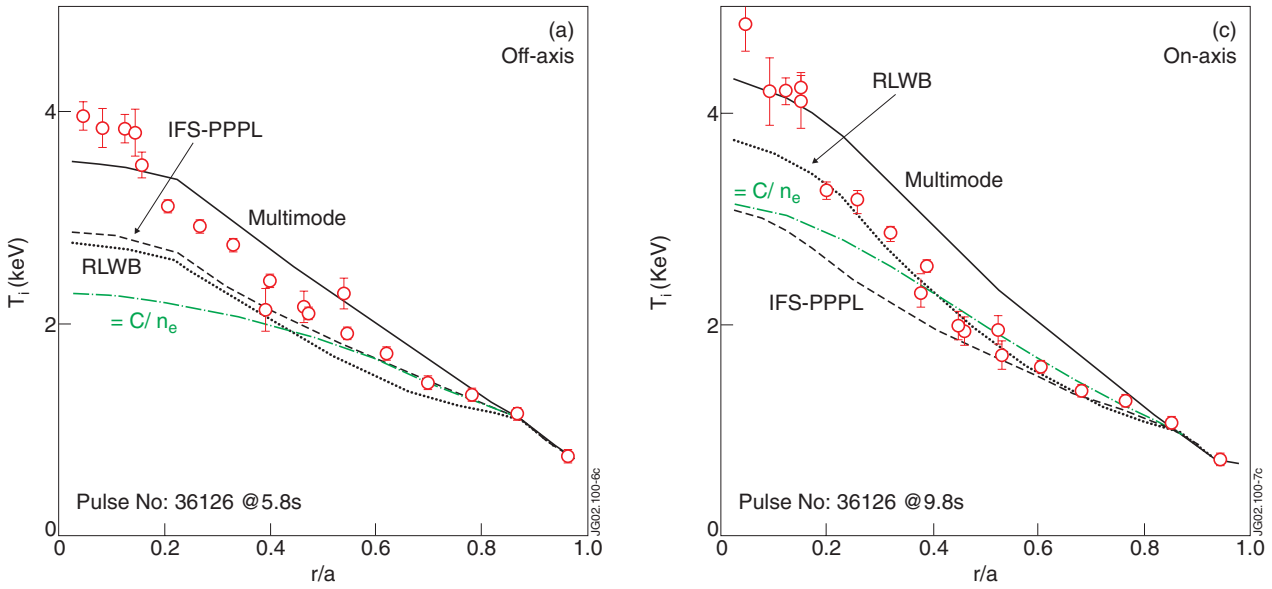

Figure 9. Measured and predicted ion temperature for plasma with off axis (a) and on-axis heating (c). Symbols with error bars are measured temperatures; curves are predictions for (dot-dash line), MMM-95 (solid line), RLW model (short-dash line), and IFS-PPPL model (long-dash line) [47].

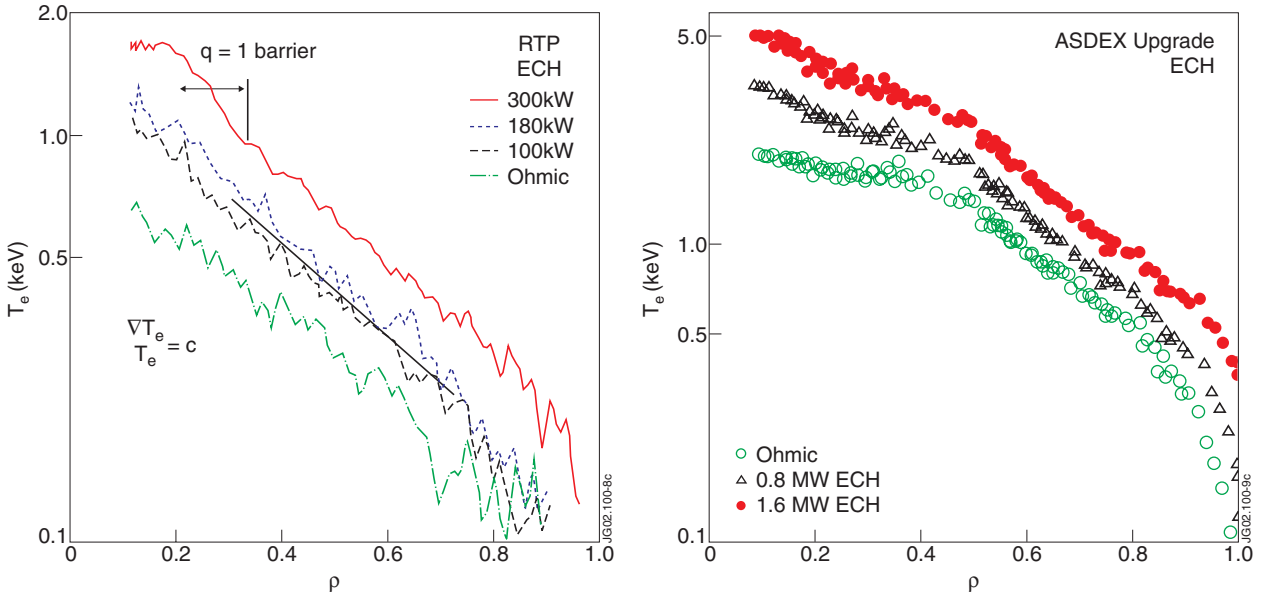

Figure 10. Electron temperature profile for a series of Ohmic and ECRH heated plasmas in RTP (left) and ASDEX-Upgrade (right) in logarithmic scale. Constant slope indicates profile stiffness [48].

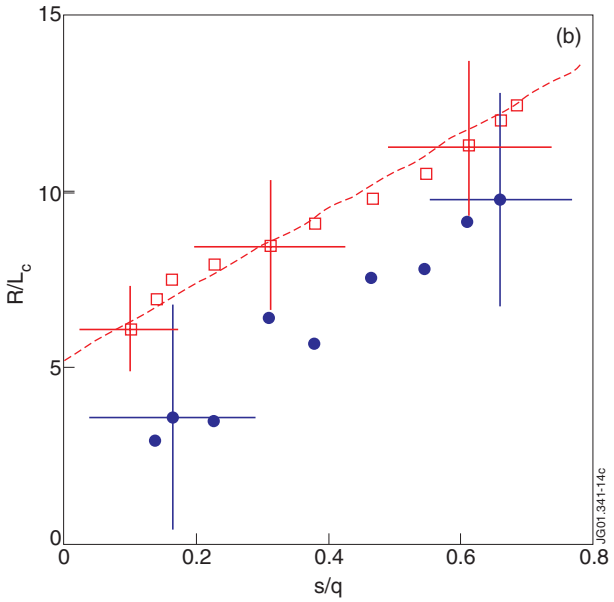

Figure11. R/L_c versus s/q (squares- power balance, circles- stability analysis, dashed line- fit) [49]

Figure 12. Simulated core and edge electron temperatures; blue diamonds corresponds to Weiland model, diamonds to IFS/PPPL, green- to GLF23 and black one to CDBM model. The lines reproduce the experimental points at low and high $T_e(0.8)$ [46].

Figure 13. Characteristic Δ contours of the ETG turbulence in the x-y plane [51]

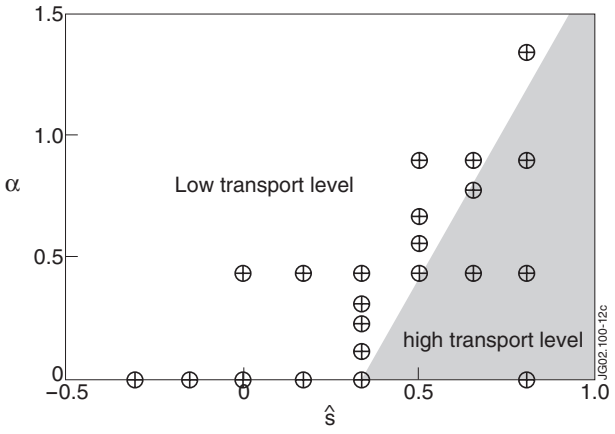

Figure 14. Non-linear simulation results for the ETG-induced transport as a function of s and ± (circles with crosses indicate strong transport) [52]

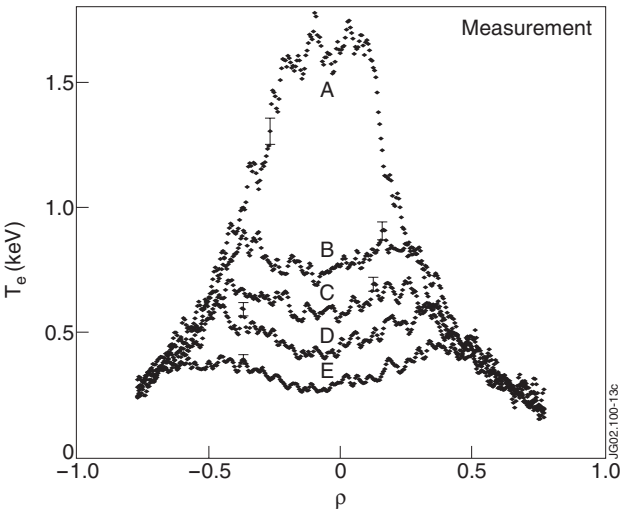

Figure 15. Measured T_e profiles in RTP with the EC resonance position shifting outward counting from A to E [58]

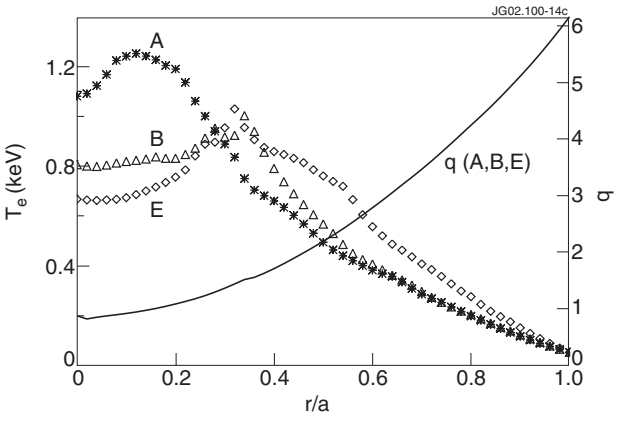

Figure 16. Calculated T_e and q profiles for the cases A, B and E from Figure 15 [60].

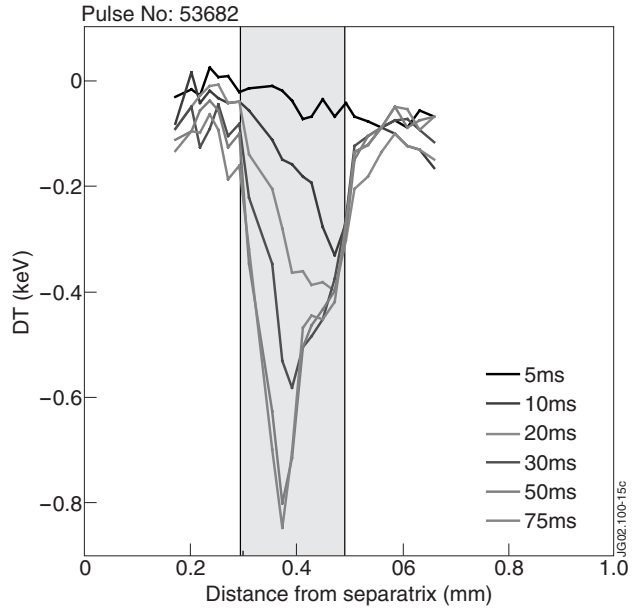

Figure 17. Time evolution of the T_e perturbation within the ITB triggered by laser ablation in Optimised Shear JET plasma (colour code indicates time after the onset of the cold pulse) [63]

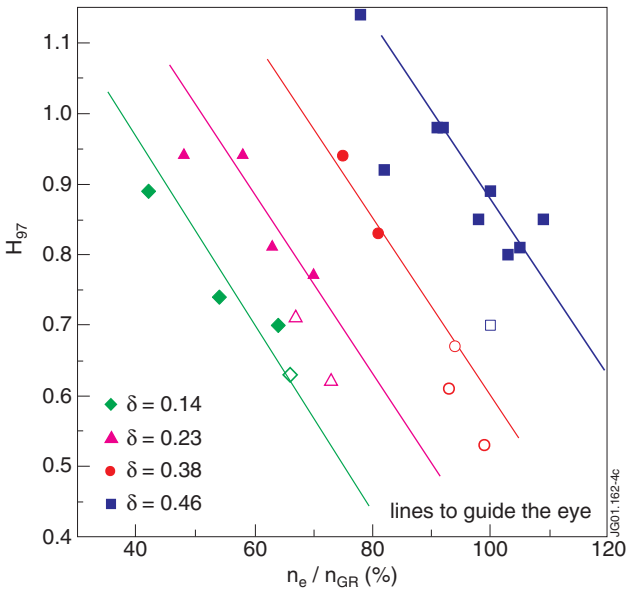

Figure 18. Confinement enhancement factor (H_{97}) as function of the Greenwald number n_e/n_{GR} for JET plasmas with different]triangularity [66]

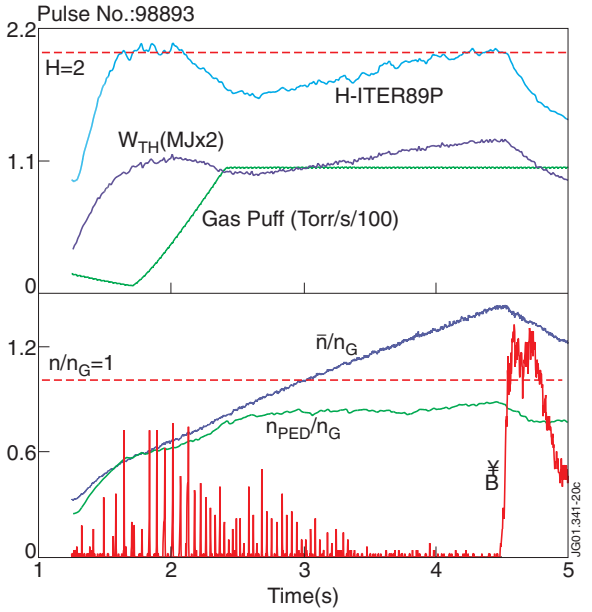

Figure 19. Time traces of plasma energy, line average and edge density, gas puff intensity and confinement characteristic for DIII-D shot with slow gas puff [72]

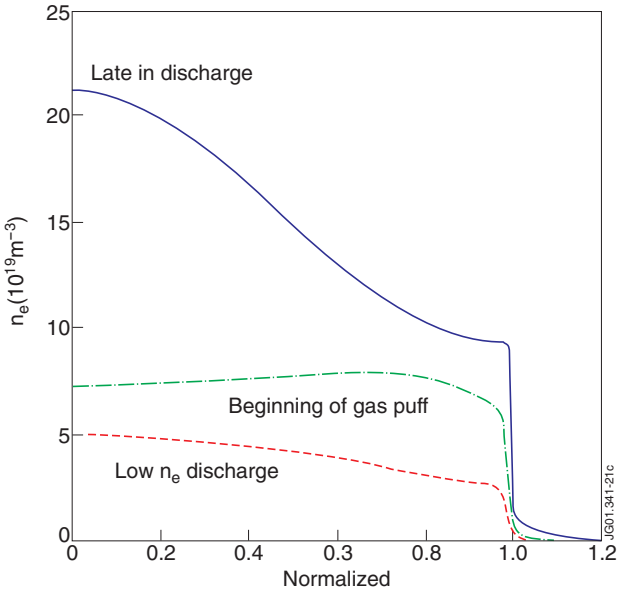

Figure 20. Time evolution of electron density profile for the same shot as in Figure 18; red curve corresponds to target density, green to the beginning of gas puff and blue to the later phase [72].

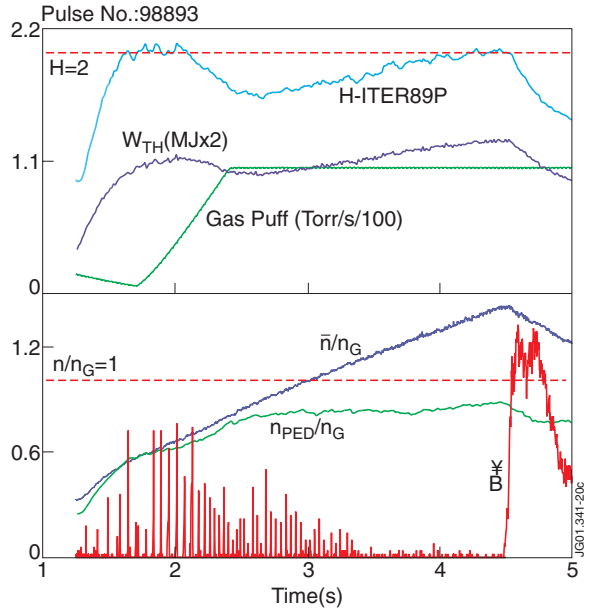

Figure 21. Density profiles at the onset of gas puff (black curve) and before the radiative collapse (red curve) in JET discharge with slow gas puff [73].

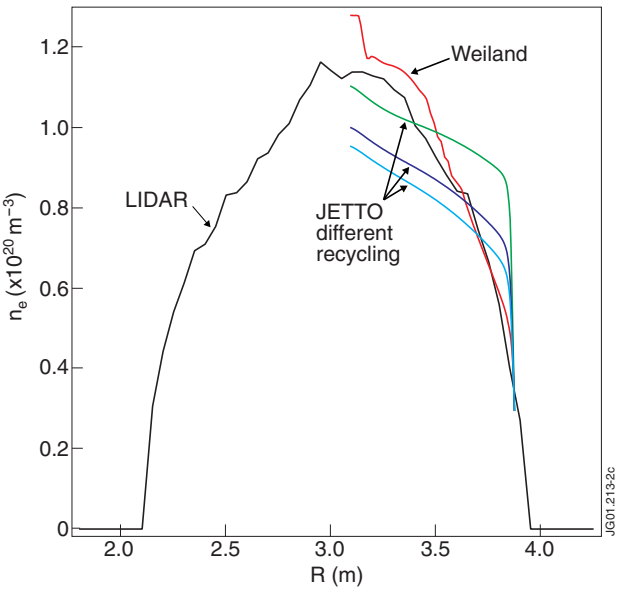

Figure 22. Measured electron density profile before collapse (black curve) and simulated with either Weiland model (red curve) or with JETTO model (three curves with different level of wall recycling) [74].